# AFRL-ML-WP-TR-2002-4018


# CLOSED FIELD UNBALANCED MAGNETRON SPUTTERING -- ENVIRONMENTALLY SAFE CORROSION AND WEAR COATINGS FOR FASTENERS

**Dr. Larry L. Fehrenbacher**

**TECHNOLOGY ASSESSMENT & TRANSFER, INC.**
**133 DEFENSE HIGHWAY, SUITE 212**
**ANNAPOLIS, MD 21401**

## FEBRUARY 2002

**FINAL REPORT FOR PERIOD OF 01 JULY 1996 – 30 JUNE 2000**

**Approved for public release; distribution unlimited.**

**MATERIALS AND MANUFACTURING DIRECTORATE**
**AIR FORCE RESEARCH LABORATORY**
**AIR FORCE MATERIEL COMMAND**
**WRIGHT-PATTERSON AIR FORCE BASE, OH 45433-7750**

# REPORT DOCUMENTATION PAGE

Form Approved OMB No. 0704-0188



| 1. REPORT DATE (DD-MM-YYYY) | 2. REPORT TYPE | 3. DATES COVERED (FROM - TO) |
|---|---|---|
| 01-02-2002 | Final rept. | 01-07-1996 to 30-06-2000 |

4. TITLE AND SUBTITLE
Closed Field Unbalanced Magnetron sputtering--environmentally Safe Corrosion and Wear Coatings for Fasteners
Unclassified

5a. CONTRACT NUMBER
F33615-96-C-5076

5b. GRANT NUMBER

5c. PROGRAM ELEMENT NUMBER

6. AUTHOR(S)
Fehrenbacher, Larry L. ;

5d. PROJECT NUMBER

5e. TASK NUMBER

5f. WORK UNIT NUMBER

7. PERFORMING ORGANIZATION NAME AND ADDRESS
Technology Assessment & Transfer, Inc.
133 Defense Highway, Suite 212
Annapolis, MD21401

8. PERFORMING ORGANIZATION REPORT NUMBER

9. SPONSORING/MONITORING AGENCY NAME AND ADDRESS
Materials and Manufacturing Directorate
Air Force Research Laboratory
Air Force Materiel Command
Wright-Patterson AFB, OH45433-7750

10. SPONSOR/MONITOR'S ACRONYM(S)

11. SPONSOR/MONITOR'S REPORT NUMBER(S)

12. DISTRIBUTION/AVAILABILITY STATEMENT
APUBLIC RELEASE
,

13. SUPPLEMENTARY NOTES

14. ABSTRACT
The Wear Sciences Coating Group of TA&T, Inc. under DARPA sponsorship has developed a new thin film coating method process aircraft piece parts such as fasteners and bearing balls.

15. SUBJECT TERMS
Cd/Cr replacement; coating; Cr CrN multilayer; environmentally compliant; friction; pollution; prevention; wear corrosion resistant

| 16. SECURITY CLASSIFICATION OF: | | | 17. LIMITATION OF ABSTRACT | 18. NUMBER OF PAGES | 19. NAME OF RESPONSIBLE PERSON |
|---|---|---|---|---|---|
| a. REPORT | b. ABSTRACT | c. THIS PAGE | Same as Report (SAR) | 40 | Fenster-EM14, Lynn<br>lfenster@dtic.mil |
| Unclassified | Unclassified | Unclassified | | | 19b. TELEPHONE NUMBER<br>International Area Code<br>Area Code Telephone Number<br>703767-9007<br>DSN<br>427-9007 |

## NOTICE

Using government drawings, specifications, or other data included in this document for any purpose other than government procurement does not in any way obligate the US Government. The fact that the government formulated or supplied the drawings, specifications, or other data does not license the holder or any other person or corporation or convey any rights or permission to manufacture, use, or sell any patented invention that may relate to them.

This report is releasable to the National Technical Information Service (NTIS). At NTIS, it will be available to the general public, including foreign nations.

This technical report has been reviewed and is approved for publication.

JEFFREY S. ZABINSKI, Chief
Nonstructural Materials Branch
Nonmetallic Materials Division

ROBERT M. SUSNIK, Deputy Chief
Nonmetallic Materials Division
Materials and Manufacturing Directorate

Do not return copies of this report unless contractual obligations or notice on a specific document requires its return.

# REPORT DOCUMENTATION PAGE

*Form Approved*
*OMB No. 0704-0188*



| 1. REPORT DATE *(DD-MM-YY)* | 2. REPORT TYPE | 3. DATES COVERED *(From - To)* |
|---|---|---|
| February 2002 | Final | 07/01/1996 – 06/30/2000 |

**4. TITLE AND SUBTITLE**
CLOSED FIELD UNBALANCED MAGNETRON SPUTTERING -- ENVIRONMENTALLY SAFE CORROSION AND WEAR COATINGS FOR FASTENERS

**5a. CONTRACT NUMBER**
F33615-96-C-5076

**5b. GRANT NUMBER**

**5c. PROGRAM ELEMENT NUMBER**
62102F

**6. AUTHOR(S)**
Dr. Larry L. Fehrenbacher

**5d. PROJECT NUMBER**
4347

**5e. TASK NUMBER**
62

**5f. WORK UNIT NUMBER**
01

**7. PERFORMING ORGANIZATION NAME(S) AND ADDRESS(ES)**
TECHNOLOGY ASSESSMENT & TRANSFER, INC.
133 DEFENSE HIGHWAY, SUITE 212
ANNAPOLIS, MD 21401

**8. PERFORMING ORGANIZATION REPORT NUMBER**

**9. SPONSORING/MONITORING AGENCY NAME(S) AND ADDRESS(ES)**
MATERIALS AND MANUFACTURING DIRECTORATE
AIR FORCE RESEARCH LABORATORY
AIR FORCE MATERIEL COMMAND
WRIGHT-PATTERSON AIR FORCE BASE, OH 45433-7750

**10. SPONSORING/MONITORING AGENCY ACRONYM(S)**
AFRL/MLBT

**11. SPONSORING/MONITORING AGENCY REPORT NUMBER(S)**
AFRL-ML-WP-TR-2002-4018

**12 DISTRIBUTION/AVAILABILITY STATEMENT**
Approved for public release; distribution unlimited.

**13. SUPPLEMENTARY NOTES**

**14 ABSTRACT** ***(Maximum 200 Words)***

The Wear Sciences Coating Group of TA&T, Inc. under DARPA sponsorship has developed a new thin film coating method to process aircraft piece parts such as fasteners and bearing balls. The objective of this technology development, demonstration, and commercialization program was to replace cadmium-plated parts with an environmentally friendly, low-cost multilayer and/or graded coating based on the Cr/CrxN system. This same material system was also evaluated as an improved bearing coating replacement for electroplated chromium. Coating performance was optimized using correlations between microstructure characterizations and fundamental mechanical, tribological, and corrosion properties of the coatings. The payoff of new environmentally benign coatings and processes that can eliminate the use of hazardous electroplated cadmium and chromium and resin-bonded dry film lubricants is enormous. Physical vapor deposited nitride coatings (especially CrxN based) offer good corrosion and wear resistance and environmental cleanliness. Nitride/metal multilayer coatings offer even better corrosion resistance, lower friction, and higher wear resistance.

**15. SUBJECT TERMS**
Cd/Cr replacement, coating, Cr CrN multilayer, environmentally compliant, friction, pollution, prevention, wear corrosion resistant

| 16. SECURITY CLASSIFICATION OF: | | | 17. LIMITATION OF ABSTRACT: | 18. NUMBER OF PAGES | 19a. NAME OF RESPONSIBLE PERSON (Monitor) |
|---|---|---|---|---|---|
| a. REPORT | b. ABSTRACT | c. THIS PAGE | | | DR. JEFFREY S. ZABINSKI |
| Unclassified | Unclassified | Unclassified | SAR | 40 | 19b. TELEPHONE NUMBER *(Include Area Code)* (937) 255-4860 |

**Standard Form 298 (Rev. 8-98)**
Prescribed by ANSI Std. Z39-18

**Table of Contents**

## I. Introduction and Background

The Wear Sciences Coating Group (WSCG) of TA&T, Inc. under DARPA sponsorship has developed a new, thin film coating method to process aircraft piece parts, such as fasteners and bearing balls. The objective of this technology development, demonstration and commercialization program was to replace cadmium plated parts with an environmentally friendly, low cost multilayer and/or graded coating based on the $Cr/Cr_XN$ system. This same material system was also evaluated as an improved bearing coating replacement for electroplated chromium. Coating performance was optimized using correlations between microstructure characterizations and fundamental mechanical, tribological, and corrosion properties of the coatings.

Fasteners and bearings are large volume, consumable components commonly used in defense and commercial applications. Yearly requirements of new and replacement parts reach astronomical proportions in the defense industry. Studies of the losses from equipment failures from mechanically related (corrosion, wear, or fatigue damage) mishaps reaches millions of dollars annually. More paramount is the loss of life in these mishaps. The payoff of new environmentally benign coatings and processes that can eliminate the use of hazardous electroplated cadmium and chromium, and resin-bonded dry film lubricants is enormous. Physical vapor deposited (PVD) nitride coatings (especially $Cr_XN$ based) offer good corrosion and wear resistance and environmental cleanliness. Nitride/metal multilayer coatings offer even better corrosion resistance, lower friction, and higher wear resistance.

## II. Technical Approach

The Wear Sciences and Coatings Group of TA&T divided the development program into several independent initiatives in order to maintain clear focus on the multiple issues involved. In most PVD coating methods, separate emphasis on developing optimized properties and sputtering methodology would not be matured separately, but thin film coating of irregularly shaped fasteners requires the tumbling of the fasteners within the coating environment which may affect the quality of an otherwise high performance film. Non-uniform exposure to the depositing species and/or non-uniform bias are the main concerns for deposition on irregularly

shaped fasteners in the barrel sputtering system. Therefore, WSCG has been using a Sloan model 1800 magnetron sputtering system to reactively sputter CrN on a variety of substrates in order to develop an optimum sputtering protocol. These analyses are presented in Section III.

Meanwhile, the oscillating barrel sputtering system was designed and improved separately throughout the program. A description of the designs and final implementation are given in Section IV.

The third front in the optimization of the $Cr_xN$ films has been conducted by TA&T's subcontractor, the University of Michigan, and has focused on the relationship between sputtering parameters in a DC sputtering mode and film morphologies and residual stresses. These sputtering trials and analyses were conducted in the University of Michigan's DC sputtering chamber. A summary of their results are given in Section V of this report.

The results and trends of the two sputtering initiatives were then combined to establish a quality, repeatable coating in the barrel oscillating deposition system. Coatings conducted in the barrel sputtering system and their analyses are described in Section VI.

## III. TA&T Coating Studies & Analysis

WSCG conducted deposition parameter, composition and physical property studies on CrN films using a Sloan model 1800 planar magnetron sputtering system. These depositions investigated the sputtering parameters' relationships to residual stress and film properties of CrN films.

Residual stress in the films were monitored by utilizing steel witness coupons included in each deposition. The residual stresses were assumed to be isotropic. The net deflection of these witness coupons provided a measure of the combined intrinsic (microstructural/chemical) and extrinsic (thermal mismatch) stresses. This net stress is an important engineering detail for final coating of parts since it influences film failure modes, coefficient of friction, wear resistance, and fatigue resistance.

Other analytical techniques are described in their respective following sections.

### III.A TA&T Sputtering Protocols & Reactive Gas Control

The initial sputtering protocols were established from literature, preliminary experiments in the barrel sputtering system, and previous successful TA&T protocols for similar metals in the Sloan 1800 system. The $Cr_xN$ protocols were then adjusted through feedback from x-ray diffraction, coefficient of friction, wear resistance, and residual stress measurements. The following table illustrates the final ranges of the parameters studied.

**Table I:** Sputtering Protocol Ranges

| Parameter | Values Studied |
|---|---|
| Target Power | 390 – 600 W |
| Target Mode | RF & DC |
| Argon:Nitrogen Ratio (via RGA) | 25:75 – 70.5:29.5 |
| Substrate Bias | 0 to –375V |
| Total Chamber Pressure | 1.5 & 2.5 millitorr |
| Target-to-Substrate Distance | 2.5 in., 3.5 in. |
| Substrate Linear Speed | 10 – 24 in/min |
| Film Overcoats | none & $MoS_2$ |

Through the feedback procedure, TA&T determined that significant variability in wear resistance and coefficients of friction were most likely due to unreliable, and therefore unrepeatable, argon to nitrogen gas ratios as determined by gas flow rates. Therefore, a standard procedure was initiated to measure the argon and nitrogen partial pressures in the chamber with a Residual Gas Analyzer (RGA) in order to increase accuracy. The use of the RGA stabilized the film screening test results.

### III.B TA&T XRD Results and the $Cr_xN$ Phase Field

X-ray diffraction was conducted by WSCG to establish the relationship between substrate bias, chromium target power, preferred orientation and crystallographic phases of the deposited CrN polycrystalline films. X-ray diffraction was conducted at WSCG with a Phillips model

1730 x-ray powder diffractometer. Typical scans were conducted at 40kV and 30mA with Cu $K_\alpha$ (1.544 Å) radiation.

All of the x-ray scans from this program were recently reevaluated for phase content. In general, it was found that with 600W target power in the Sloan system the films were almost always mixed phase character, CrN and $Cr_2N$. By increasing the nitrogen partial pressure to high levels (75%) $Cr_2N$ could be produced without CrN present. However, with such high nitrogen levels, the deposition rate decreased significantly because of the lower Ar content, which is the efficient sputtering gas.

Also, films with dominant $Cr_2N$ character were often found with $Cr_2O_3$. It is believed that, as the films were put down with excess chromium, the chromium rich $Cr_2N$ phase was favored but also pure chromium phase was also put down. Subsequently, oxidation of the Cr phase occurred immediately upon removal from the vacuum chamber. $Cr_2O_3$ is a lubricious oxide and may have contributed to some of the low friction values measured for bare $Cr_xN$ films, indicated in Section III.C.

One other trend observed was that DC sputtered films were generally oriented with $Cr_2N$ (10·0) out-of-plane texture, while RF deposited films were not oriented. Previously reported oriented RF deposited films were incorrectly indexed with a $Cr_2O_3$ peak mistaken for an oriented peak.

### III.C Residual Stress and Coefficient of Friction

Characterization of the CrN films included friction and wear testing. Friction and wear tests were conducted with a pin-on-disk type arrangement, as seen in Figure 1. A 7/64 in. diameter WC-Co ball served as the usual counterface. Normal loading of 2.0kg (19.6N) was applied to the system. This corresponds to an initial Hertzian contact stress of 450GPa. Force transducers mounted on the pin assembly measured the forces while the test ball remained in contact with the surface of the rotating sample. The acquired voltage data from the transducers were decoupled, then translated to corresponding coefficient of friction ($\mu_f$) values. Adhesion and wear were also recorded via optical measurements of the sample wear scar widths and the

corresponding wear patch on the test balls, ex situ. All friction and wear measurements were conducted on films on AISI 52100 heat treated substrates.

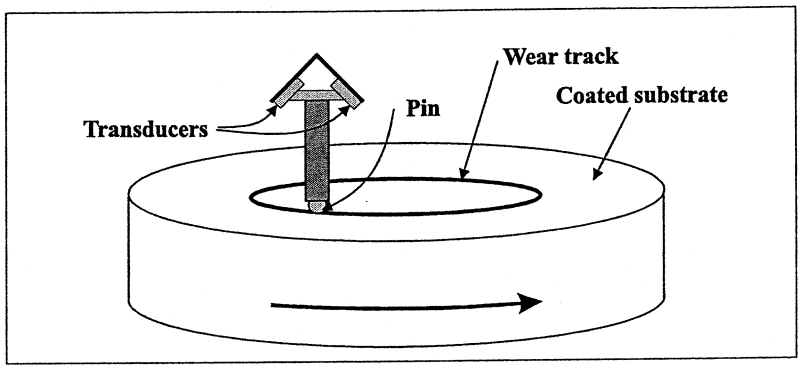


**Figure 1:** Pin-on-disk friction and wear test.

For bearing applications, it was not expected that the bare CrN surface would be sufficiently low friction. However, $MoS_2$ has often yielded low coefficients of friction because of its laminar crystal structure (similar to graphite), especially on hard ceramic substrates.[1] Therefore, many $MoS_2$ overcoats were applied to the Sloan $Cr_xN$ films to lower the coefficients of friction. Figure 2 shows the effects of compressive residual stress on the film coefficients of friction for RF deposited CrN, bare and $MoS_2$ overcoated, and DC deposited CrN, bare and $MoS_2$ overcoated.

[1] Williams B.J., E.W. Roberts, W.B. Price. "Ultra-Low-Friction Films on Modified Surfaces." Final Technical Report for The European Office of Aerospace Research and Development, January 1990.

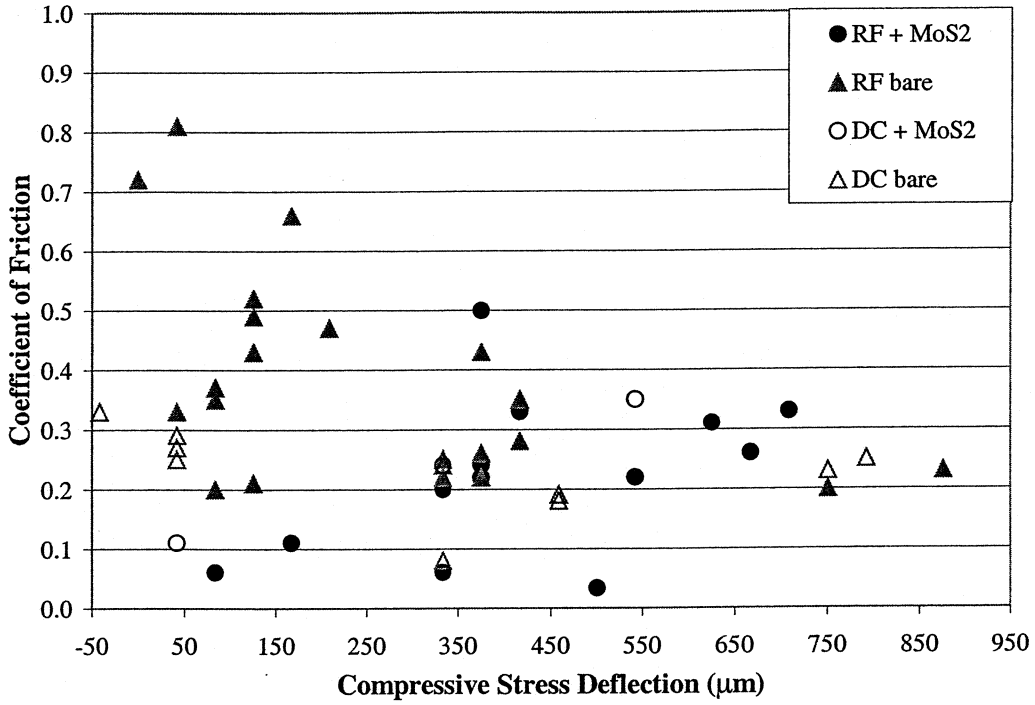


**Figure 2:** Effect of residual stresses on coefficients of friction of Sloan $Cr_xN$ films deposited RF, DC, and overcoated with $MoS_2$.

There is significant scatter of the data in Figure 2 because of varying deposition parameters among the runs. Therefore, within each category of films there are slight differences in film thicknesses, phase content, and surface morphology. However, several trends are still visible.

Firstly, it is clear from the figure that both overcoated and bare coatings, deposited by RF or DC magnetron sputtering, all converge to coefficients of friction between 0.2 and 0.3 at high compressive residual stresses. At such high stresses, primarily due to significant argon ion peening effects, the $Cr_xN$ films are highly densified, hard, and smooth on the surface. Therefore, the mode of deposition (DC or RF) is not the significant factor determining the surface morphology or coefficient of friction, and 0.2 to 0.3 is the natural coefficient of friction between $Cr_xN$ and WC-Co. Also, $MoS_2$ overcoats were unexpectedly insignificant in reducing the coefficients of friction at these high stress levels. We believe this is due to the extremely hard, smooth $Cr_xN$ underlayer surface. Since the applied loads during the tests were significantly

above the yield point of $MoS_2$, the test pins ploughed through the $MoS_2$ in just a few cycles, eventually riding on bare $Cr_xN$ and showing ultimate coefficients of friction to the bare $Cr_xN$ tests.

Secondly, both RF and DC deposited bare $Cr_xN$ coatings (triangle symbols) trend to higher coefficients of friction at lower compressive residual stresses. This is expected since the lower compressive stress films are relatively more porous and rough on the surface due to less ion peening action. Therefore, surface asperities may catch and break off during pin-on-disk testing, producing third body wear particles and greater coefficients of friction. It is interesting to note, however, that the coefficients of friction of DC bare coatings are much less dependent on stress than the RF deposited coatings.

Lastly, both the RF and DC $Cr_xN$ coatings with $MoS_2$ overcoats (circle symbols) trend in the opposite direction as that of the bare coatings. That is, the $MoS_2$ overcoated films trend to lower coefficients of friction with lower compressive residual stress. This effect was unexpected, but it is clear now that the relatively more porous films at lower compressive residual stress give much better physical bonding of the $MoS_2$ coatings as well as provide micropockets subsequently filled with $MoS_2$. Therefore, even when the applied test loads were greater than the $MoS_2$ yield strength, the $MoS_2$ coating could resist ploughing due to interlocking physical bonding. Additionally, even as $MoS_2$ is ploughed away from the upper surface, replenishing pockets of the lubricating film were still available in the $Cr_xN$ film to replenish the upper level film and transfer film, resulting in lower overall coefficients of friction for long times. The lowest coefficients of friction during this program were achieved with low to intermediate compressive residual stress in $MoS_2$ overcoated RF deposited $Cr_xN$.

### III.D Residual Stress and Wear Resistance

As mentioned in the previous section, optical measurements were made, ex situ, on the pin-on-disk tested films. The wear scar width on the disk was taken as a proportional measure of wear volume. Therefore, an analysis of the effects of residual stress on the wear resistance of the $Cr_xN$ films could be made using this testing procedure.

No trends are evident between residual stress and wear scar width measurements.

### III.E Coating Salt Bath Tests

A salt bath test was conducted to qualitatively evaluate the $Cr_xN$ film corrosion resistance. Films deposited on AISI 52100 bearing steel were submerged in a supersaturated aqueous NaCl solution at room temperature for two weeks. At the end of this period, the samples were removed and evaluated for corrosion. The backs of the 52100 steel substrates showed significant corrosion and rust scale. Meanwhile, corroborating literature reports of CrN resistance to corrosion, all films showed no corrosion damage or pitting.

## IV. Barrel Sputter Coater Design and Construction

The final configuration of the barrel sputter coating system is shown in Figure 3. Vacuum, gas control, motion, and magnetron control systems were assembled early in the program. The system uses a chromium target 14.5 in. x 3 in. controlled by a pulsed DC power unit operating at 20kHz. The substrate sheets are at a fixed target-to-substrate distance of 4 inches. Effective target-to-substrate distance is reduced by large part sizes.

**Figure 3:** The barrel sputter coater system – final configuration.

The most significant challenge during construction of the barrel system was the bias distribution system. The barrel sputter coater bias distribution system underwent several design

changes resulting in modified power feedthru and slip ring assemblies. The modified configuration employs copper tubing and a custom slip ring, and new feedthru design.

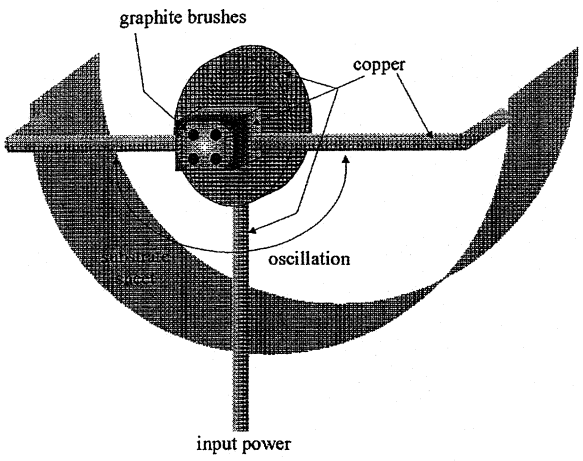


**Figure 4:** Custom slip assembly for RF bias power delivery.

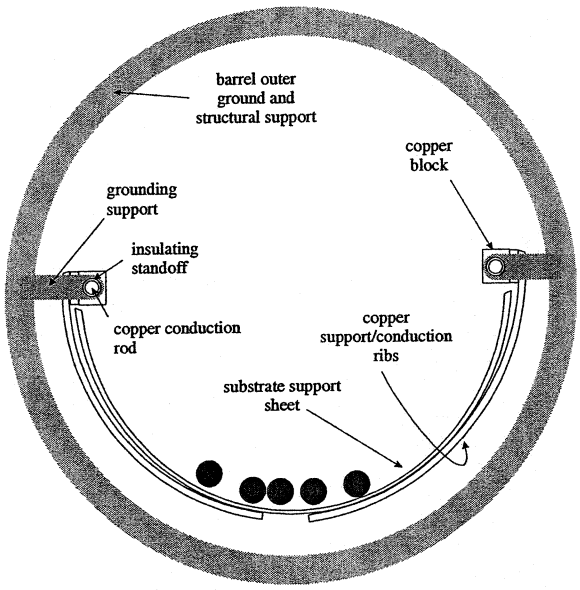


**Figure 5:** Oscillating barrel support and bias/etch power delivery structure.

Figure 4 depicts the custom slip assembly design. The slip assembly is freestanding in the chamber, supported only at the bottom of the chamber near the input end and at two locations on the rotating barrel. Rotating electrical contact is achieved by a copper block with spring loaded graphite brushes bearing against a flat copper disk. The entire power delivery system is shielded with alumina spacers and a combination of copper and stainless steel grounding in order to quench any plasma that might form along its length. This guarantees power delivery to the substrate support sheet and bias plasma forming at the parts to be coated.

Testing of this new slip assembly revealed the need for a more electrically isolated, structural substrate support sheet. The final design for this new substrate support sheet is shown schematically in Figure 5.

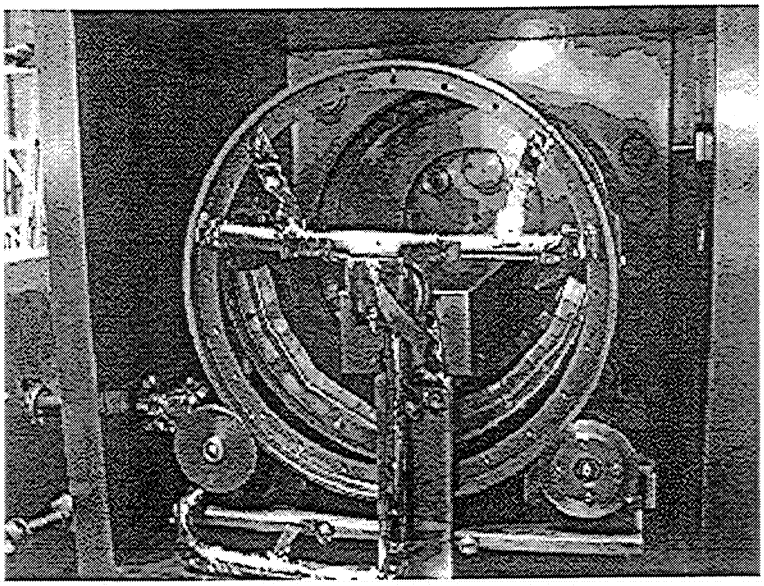

**Figure 6**: Photo of the barrel support and power delivery system.

Modifications to the substrate supports also were necessary. Previous substrate supports utilized alumina fasteners and standoffs in multiple locations to achieve the electrical isolation of the substrate support sheets. However, despite being shielded from most of the target flux these connection points were eventually coated, providing a conductive path between the ground and the biased substrate support sheets. At this point the barrel assembly would have to be disassembled and cleaned of undesirable coating. The final design objective was to eliminate these standoff connection points, and thus the possibility of a conductive path, while maintaining a well supported substrate sheet.

This goal was accomplished by reinforcing the power delivery arms to become the only support for the sheets, thus providing an air gap between the substrate support sheets and the grounded barrel frame. The design employs copper rods for power input and delivery to the substrate support sheet. These rods also provide structural support for the design while maintaining a high surface area for RF (surface running) power delivery. As seen in Figure 5, the design is freestanding within the confines of the outer, grounded structural barrel. The structural load transfers from the outer barrel through a single set of isolation standoffs within

the arms and from there into the copper rods, themselves. From there, load is supported through a pair of assembly blocks and a set of copper ribs under the substrate support sheets. All copper exposed in the figure is actually shielded with stainless steel. These shields are biased, just as the substrate support sheet, but they have a significantly lower sputtering rate than exposed copper. This protects the coatings from significant contaminants.

This design modification allowed unlimited deposition time and number of runs, which was previously defined by the time for a conductive film path to develop on the alumina standoffs. It also eliminated the need for major cleaning of the substrate support sheets. The completely redesigned barrel system is shown in Figure 6. While oscillating the barrel with the new air gap configuration, power levels up to 1750W were applied without difficulties. With the biasing difficulties resolved, oscillating deposition characterization and, ultimately, the coating of tumbling fasteners were conducted in the barrel deposition system.

## V. University of Michigan Deposition Results & Discussion

TA&T's subcontractor, the University of Michigan, conducted CrN depositions with a DC powered chromium target and without substrate biasing, as indicated in Figure 7. The University of Michigan conducted synchrotron Glancing Incident X-ray Scattering (GIXS), residual stress measurements by Double Crystal Diffraction Topography (DCDT) and the Laser Scanning Technique (LST), x-ray diffraction, x-ray texture studies, TEM, AFM, and SEM analysis of their own and TA&T samples.

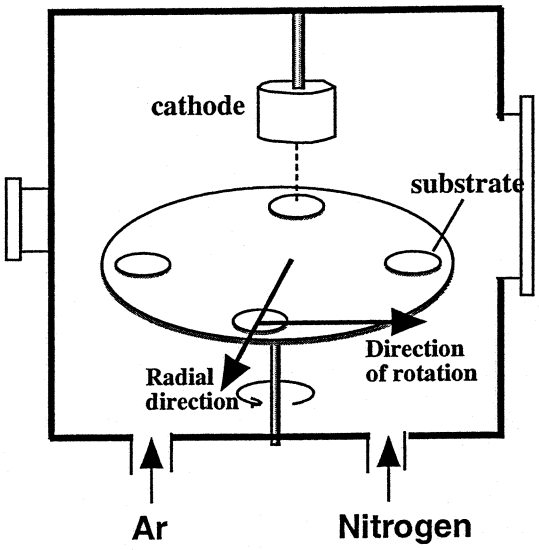


**Figure 7:** Deposition geometry used at the University of Michigan for reactive $Cr_xN$ depositions.

Michigan has conducted a series of $Cr_xN$ depositions with varying $N_2$ working gas flows from zero to 70 sccm. Depositions were conducted with a constant initial argon backfill pressure of 2.0 mTorr pressure (constant flow throughout run) and 460W Cr target power. The target-to-substrate distance for these depositions was 6cm (2.36 in). No bond layers were deposited. Control of the working gases during the depositions was conducted via gas flows only, since that system is not equipped with a Residual Gas Analyzer. With the constant argon backfill, the higher $N_2$ flow depositions were performed at higher overall chamber pressures. The pressure/flow relationships are indicated in Table II.

**Table II:** Michigan Flow/Pressure Relationships

| $N_2$ Flow (sccm) | Ar Flow (sccm) | Total Chamber Pressure (mTorr) |
|---|---|---|
| 0 | 19 | 2.00 |
| 5 | 19 | 2.23 |
| 10 | 19 | 2.48 |
| 18 | 19 | 2.80 |
| 25 | 19 | 3.08 |
| 32 | 19 | 3.50 |
| 41 | 19 | 4.05 |
| 55 | 19 | 4.75 |
| 70 | 19 | 5.40 |

## V.A DCDT Residual Stress Measurements

Through DCDT measurements at systematic azimuthal angles across the deposited films, the University of Michigan found that the residual stresses in chromium films were generally anisotropic. Further, they found that the principal stresses in the films (the maximum and minimum stresses) were directly related to the film deposition geometry and subsequent film morphology. Referring to Figure 7, U. Michigan found that the maximum (tensile) stress in Cr films was always aligned with the radial direction, while the minimum stress (also tensile) was aligned with the direction of rotation.

Zhibo Zhao at Michigan, under this program funding, has developed a new set of analytical relations, similar to Stoney's equation[2] for isotropic stresses, to relate film and substrate properties to anisotropic stresses. As a summary of the results, the relationship between the principal stresses $\sigma_1$ and $\sigma_2$ and the corresponding principal radii of curvature $R_1$ and $R_2$ on a single crystal, cubic structure substrate was shown to be:

$$\sigma_1 = \frac{1}{6}\left[\left(\frac{1}{R_1}+\frac{1}{R_2}\right)\frac{1}{2(s_{11}+s_{12})}+\left(\frac{1}{R_1}-\frac{1}{R_2}\right)\sqrt{\frac{\cos^2 2\alpha}{4(s_{11}-s_{12})^2}+\frac{\sin^2 2\alpha}{s_{44}^2}}\right]\frac{t_s^2}{t_f} \qquad (1)$$

[2] Stoney G.G. Proc. R. Soc. London Ser. A82 1729 (1909)

$$\sigma_2 = \frac{1}{6}\left[\left(\frac{1}{R_1}+\frac{1}{R_2}\right)\frac{1}{2(s_{11}+s_{12})} - \left(\frac{1}{R_1}-\frac{1}{R_2}\right)\sqrt{\frac{\cos^2 2\alpha}{4(s_{11}-s_{12})^2}+\frac{\sin^2 2\alpha}{s_{44}^2}}\right]\frac{t_s^2}{t_f} \qquad (2)$$

where:

$s_{11}$, $s_{12}$, $s_{44}$ are the compliance tensor components of the cubic crystal substrate

$t_s$ is the thickness of the substrate

$t_f$ is the thickness of the film

$\alpha$ is the angle between the [100] direction of the cubic structure substrate and $R_1$

Equations (1) and (2) reduce to Stoney's equation when the principal radii of curvature are identical, i.e. the isotropic situation[3]. The angle $\theta$ between the principal stress $\sigma_1$ and the [100] direction of the cubic structure substrate was shown to be related to the angle $\alpha$ by:

$$\tan 2\theta = \frac{2(s_{11}-s_{12})}{s_{44}}\tan 2\alpha \qquad (3)$$

Meanwhile, the $Cr_xN$ films deposited at Michigan were much closer to isotropic stress. Figure 8 shows the average film stress as a function of nitrogen flow for the $Cr_xN$ films. In general, sputtering without a negative substrate bias will result in more tensile residual stress with higher working gas pressure. This is the result of less Ar+ peening and the increase in target atom-argon ion gas phase collisions at higher pressure. Interestingly, as seen in Figure 8, DCDT on the Michigan films reveals the opposite trend, less tensile residual stress with increasing $N_2$ flow (and corresponding pressure). Note that positive values represent tensile residual stress in Figure 8. Another interesting feature is the repeatable compressive stress attained in the films at a $N_2$ flow rate of about 18 sccm. This stress valley is not fully understood, but it is corroborated by several recent studies[4,5] and is undoubtedly associated with

---

[3] Zhoa Z. "Evolution of Microstructure and Residual Stress in Sputtered Cr and $Cr_xN_y$ Thin Films" Ph.D. Dissertation, University of Michigan, Materials Science and Engineering Department, 1999.

[4] Beuien H. J. Maushart, M. Meyer, R. Suchentrunk. Mat. Sci. & Eng. A139 126 (1991)

[5] He X.M., N. Baker, S. Grigull, K.C. Walter, M.A. Nastasi. presented at MRS 1998 Fall Meeting, Boston, MA, Nov 30 – Dec 4, 1998.

the film microstructure. X-ray diffraction and TEM studies of these films revealed that these films had grain sizes on the order of 10nm (nanocrystalline), dissimilar from all of the other films deposited.

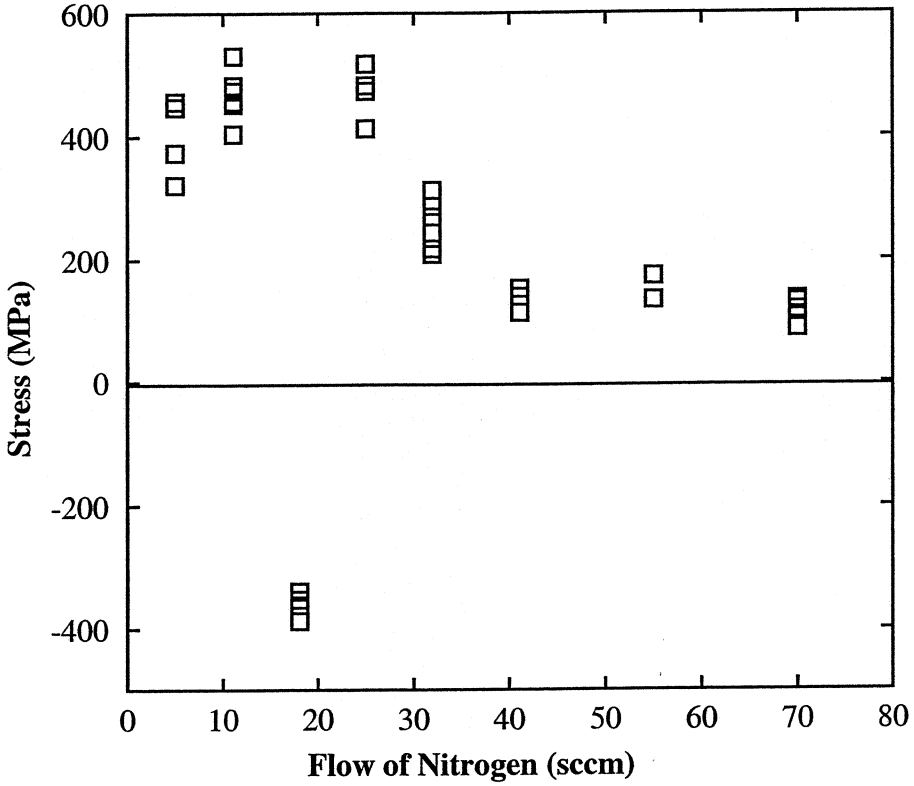


**Figure 8:** DCDT results on the residual stresses in the films deposited at 460 W, 2 mTorr Ar and various nitrogen flows. All the films have the same nominal thickness: 1μm. Positive is tensile stress.

### V.B X-Ray Diffraction Results

Michigan has used Glancing Incidence X-ray Scattering (GIXS) to analyze the phase content of their films. The scans are presented in Figure 9.

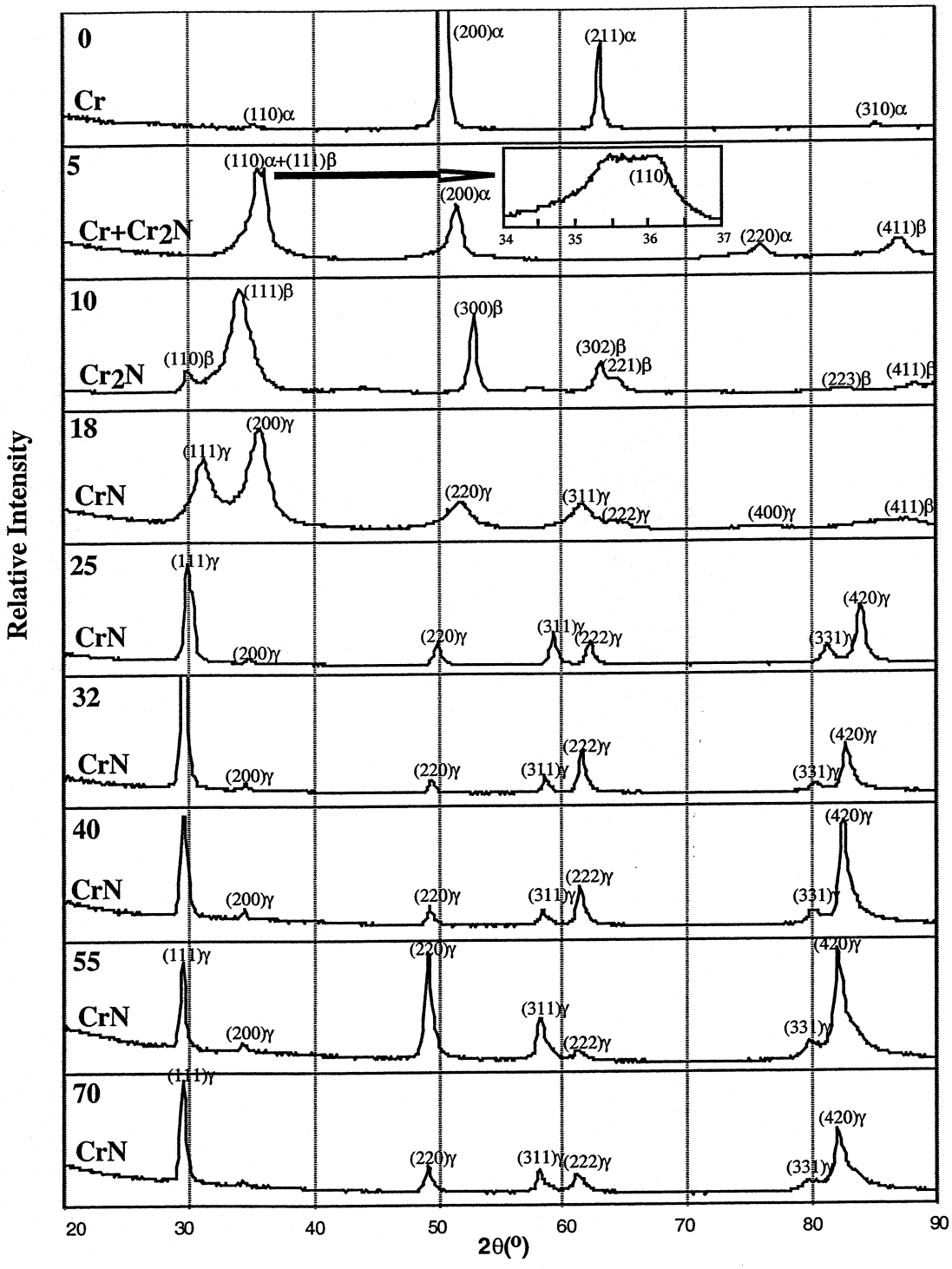


**Figure 9:** GIXS data of chromium nitride films deposited at 460 W, 2mT Ar plus various nitrogen flows.

Figure 9 clearly shows the relationship between the $Cr_xN$ phase content and the $N_2$ flow (concentration). At 10 sccm $N_2$ flow rate, the films are pure $Cr_2N$. At higher flows between 18 and 25 sccm the films convert to CrN.

The diffraction peaks of pure CrN films shift with increasing $N_2$ flow, as shown in Figure 9. The lattice parameter of the CrN can be calculated from the peak shifts. These are presented in Figure 10. Based on the lattice parameter of bulk, stoichiometric CrN, which is 4.14Å, the majority of the Michigan coatings appear to be super-stoichiometric in nitrogen. The excess nitrogen in the $CrN_{1+x}$ crystals expands the lattice because of interatomic forces. This same trend has been seen in reactively sputtered TiN where excess $N_2$ fills in tetrahedral sites in the lattice. The other phenomena that usually contributes to larger lattice parameters in sputtered films is excess implanted Ar. This usually occurs with films that are deposited under negative substrate bias; however, the Michigan films were deposited with no substrate bias. The CrN and implanted Ar concentrations could be quantified using ion sputtering XPS analysis.

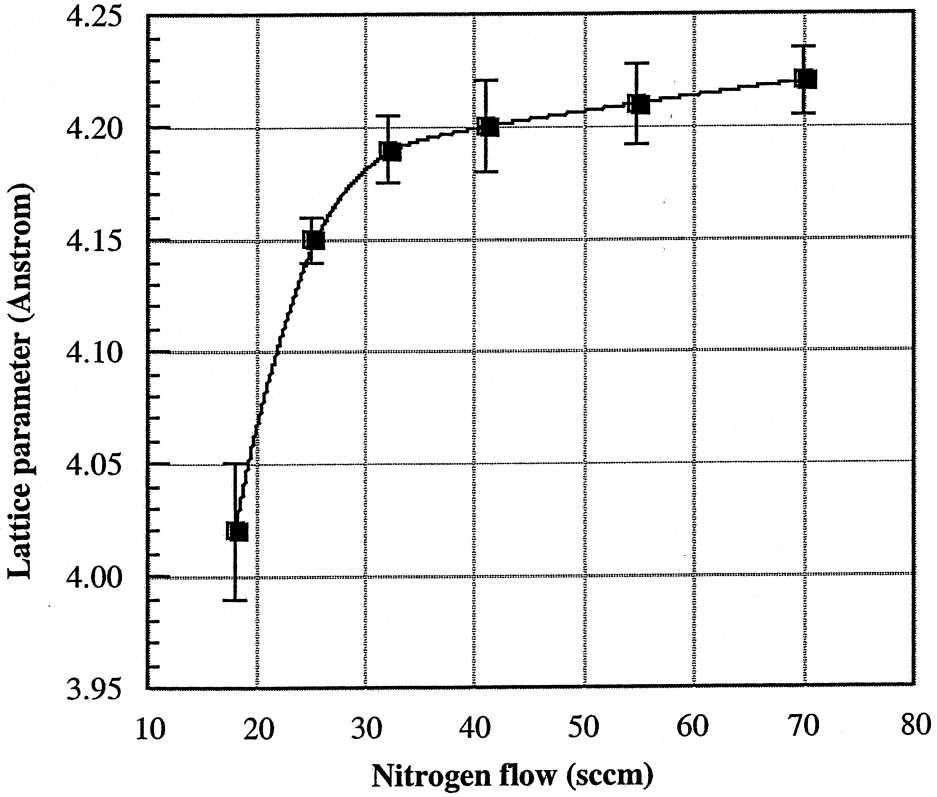


**Figure 10:** The lattice parameters of cubic $CrN_{1+x}$ as a function of nitrogen flow.

Interestingly, as seen in the XRD scans in Figure 11 and Figure 12, the majority of CrN coatings deposited in the CrN phase field are (111) out-of-plane oriented despite the lack of substrate biasing. Figure 13 shows the full pole figure for the CrN coating deposited with 32 sccm $N_2$.

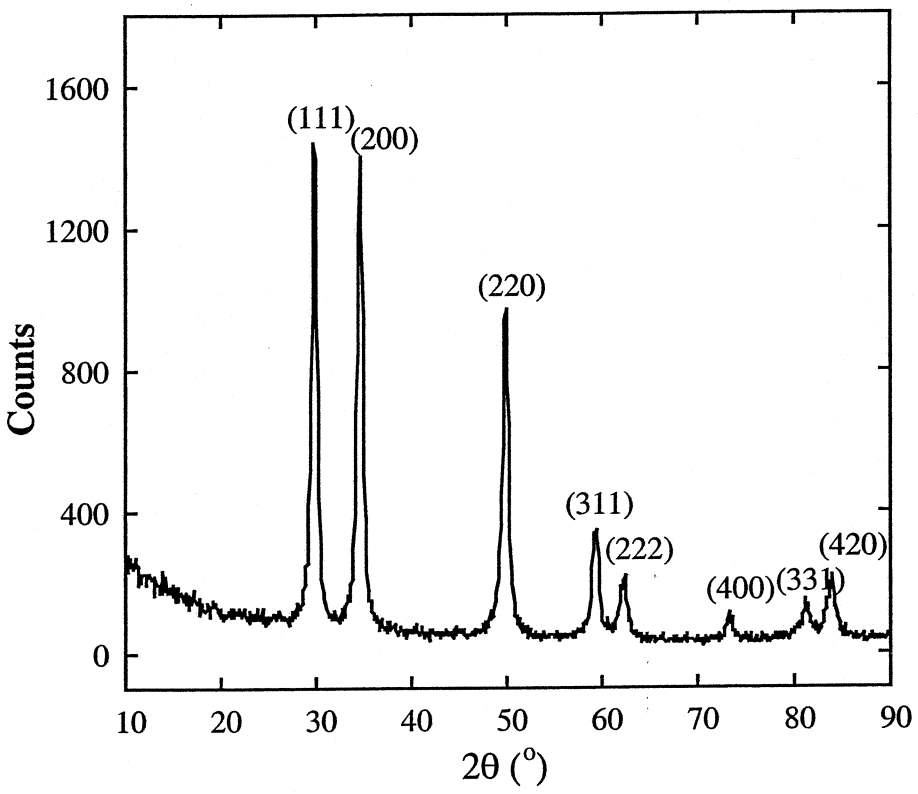


**Figure 11:** Diffraction pattern of a 60-nm film deposited at 2 mTorr Ar and 25 sccm nitrogen flow.

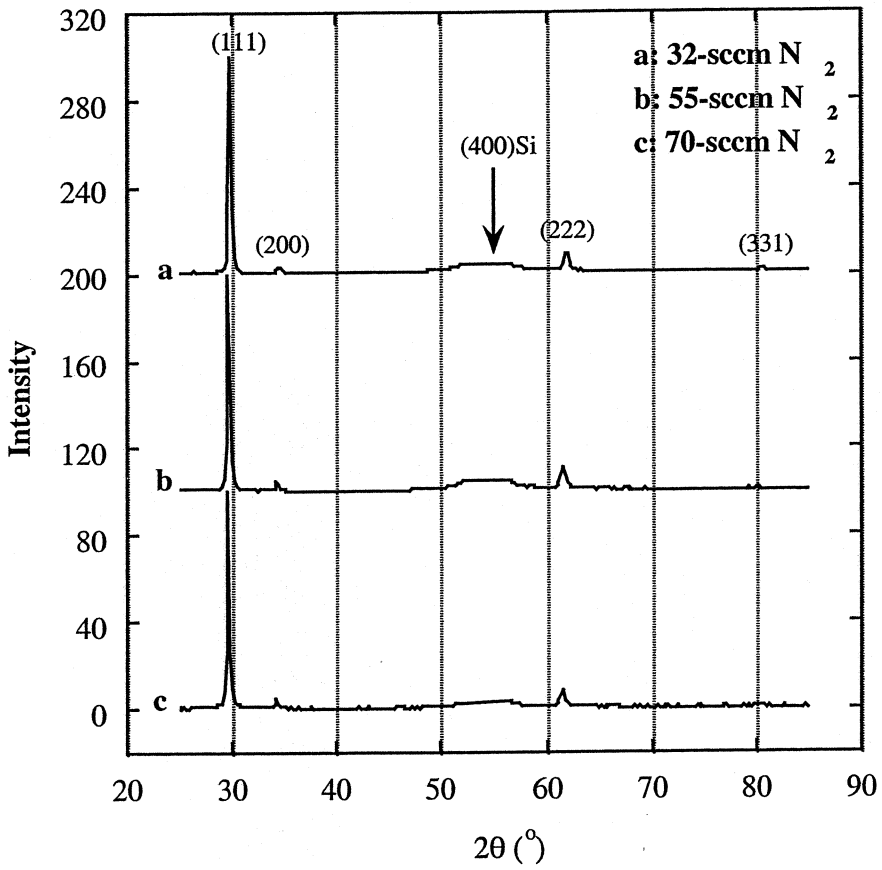


**Figure 12:** Examples of x-ray diffraction patterns showing that the CrN films deposited at high nitrogen flow have (111) *out-of-plane* texture.

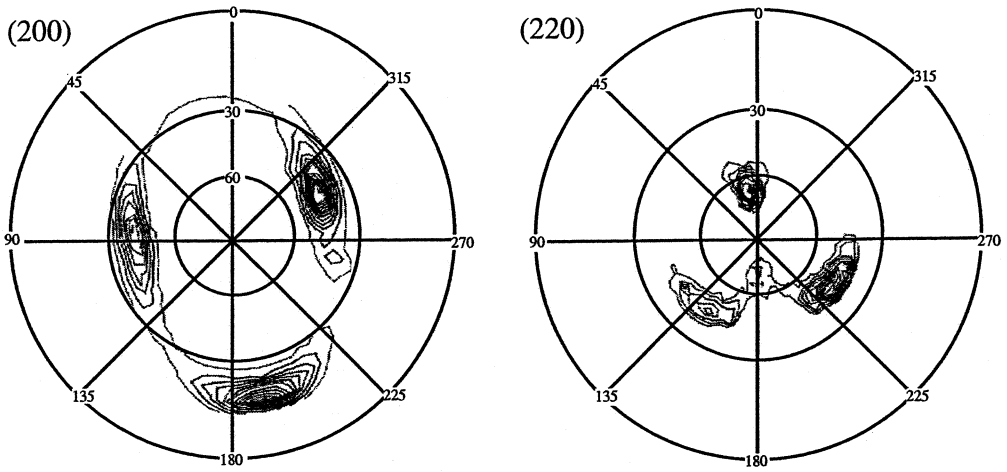


**Figure 13:** Pole figures of the (200) and (220) poles from a 1 μm thick 32-sccm film, showing the (111) *out-of-plane* texture (3-fold symmetry) and the associated *in-plane* texture.

## V.C TEM and AFM Microstructure Analysis

Michigan has conducted microstructural analyses of their films via TEM and AFM. Figure 14 shows the TEM bright field images from their films as a function of $N_2$ flow rate. The only films which show no in-plane texture are those deposited at 10 sccm (Figure 14c), 18 sccm (Figure 14d), and possibly 5 sccm (Figure 14b). These films exhibit a random nanocrystalline grain structure. The presence of mixed phases in the 5, 10, and 18 sccm films may account for the random grain growth pattern. The general in-plane texture of the other films arises from the rotation direction of the substrates under the sputtering target, and the stacking restrictions imposed by the (111) out-of-plane texture already discussed. The grains are elongated in the radial direction and compressed in the direction of substrate motion.

In-plane morphological texture is again visible in the plan AFM images of Figure 15. The morphologies of the 5 and 15 sccm $N_2$ films are much smoother than the films grown with the higher $N_2$ flow rates. The increasing peak-to-valley heights of the CrN films grown from 25 sccm $N_2$ to 40 sccm $N_2$ to 70 sccm $N_2$ is consistent with the increased (111) out-of-plane texture growth.

(a): O sccm $N_2$: Cr

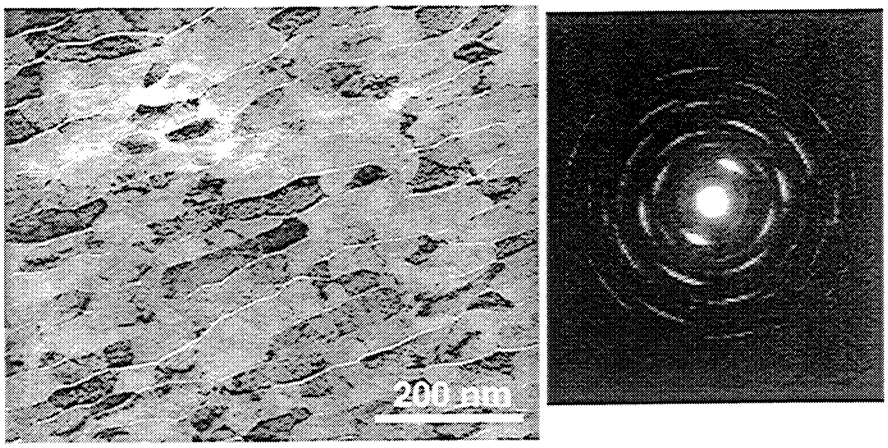


(b): 5 sccm $N_2$: Cr+$Cr_2N$

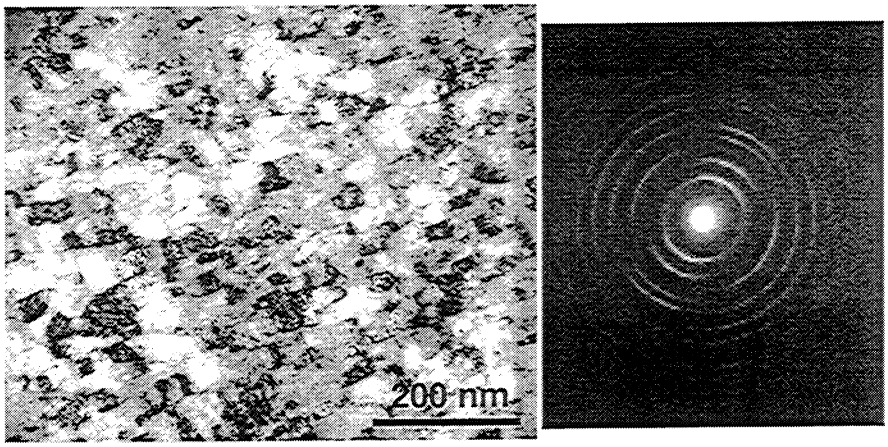


(c): 10 sccm $N_2$: $Cr_2N$

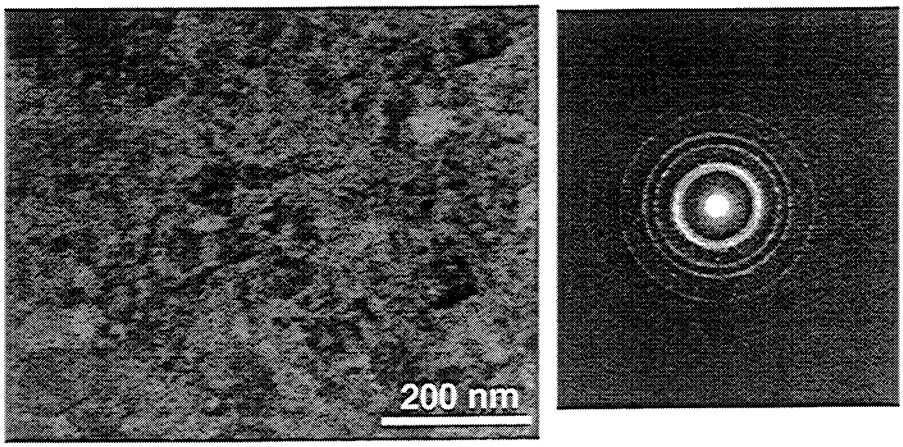


**Figure 14:** Bright field TEM images and corresponding diffraction patterns of $Cr_xN$ films at varying nitrogen flows.

(d): 18 sccm $N_2$: $CrN_x$

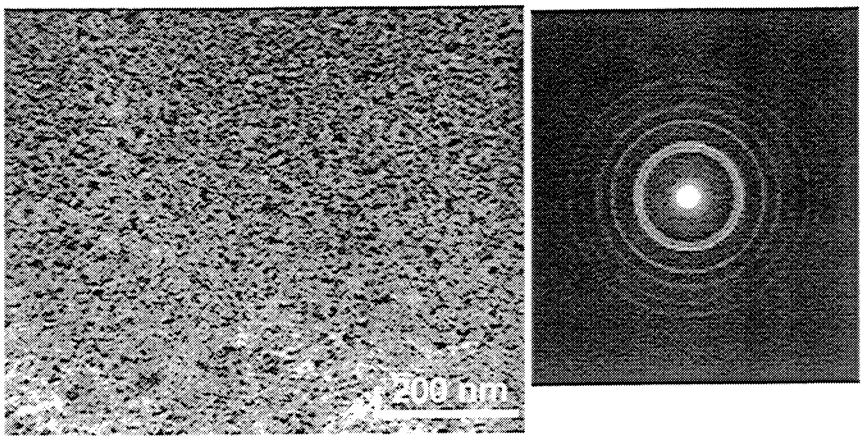


(e): 32 sccm N2: CrN

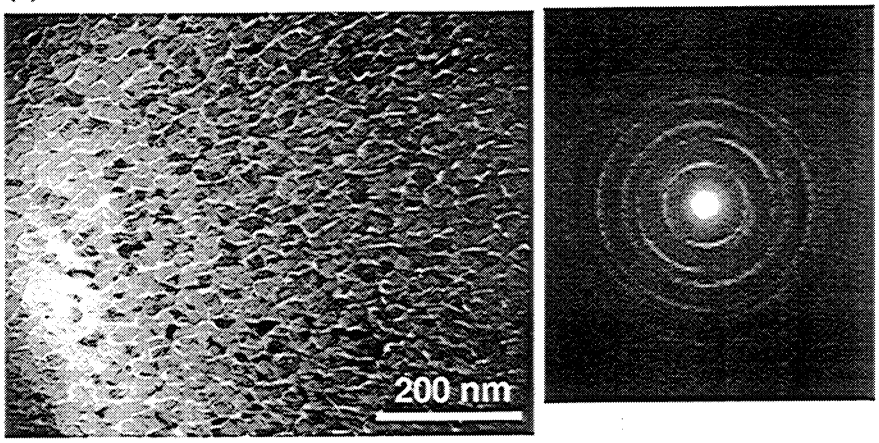


(f): 70 sccm $N_2$: CrN

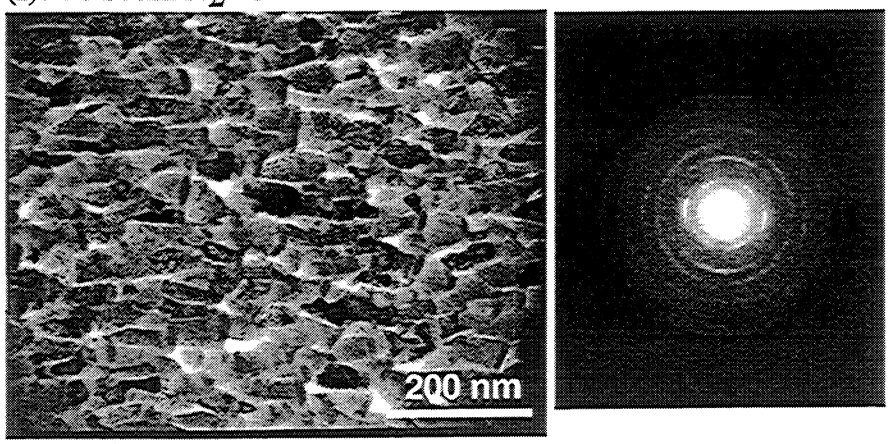


**Figure 14 (cont):** Bright field TEM images and corresponding diffraction patterns of $Cr_xN$ films at varying nitrogen flows.

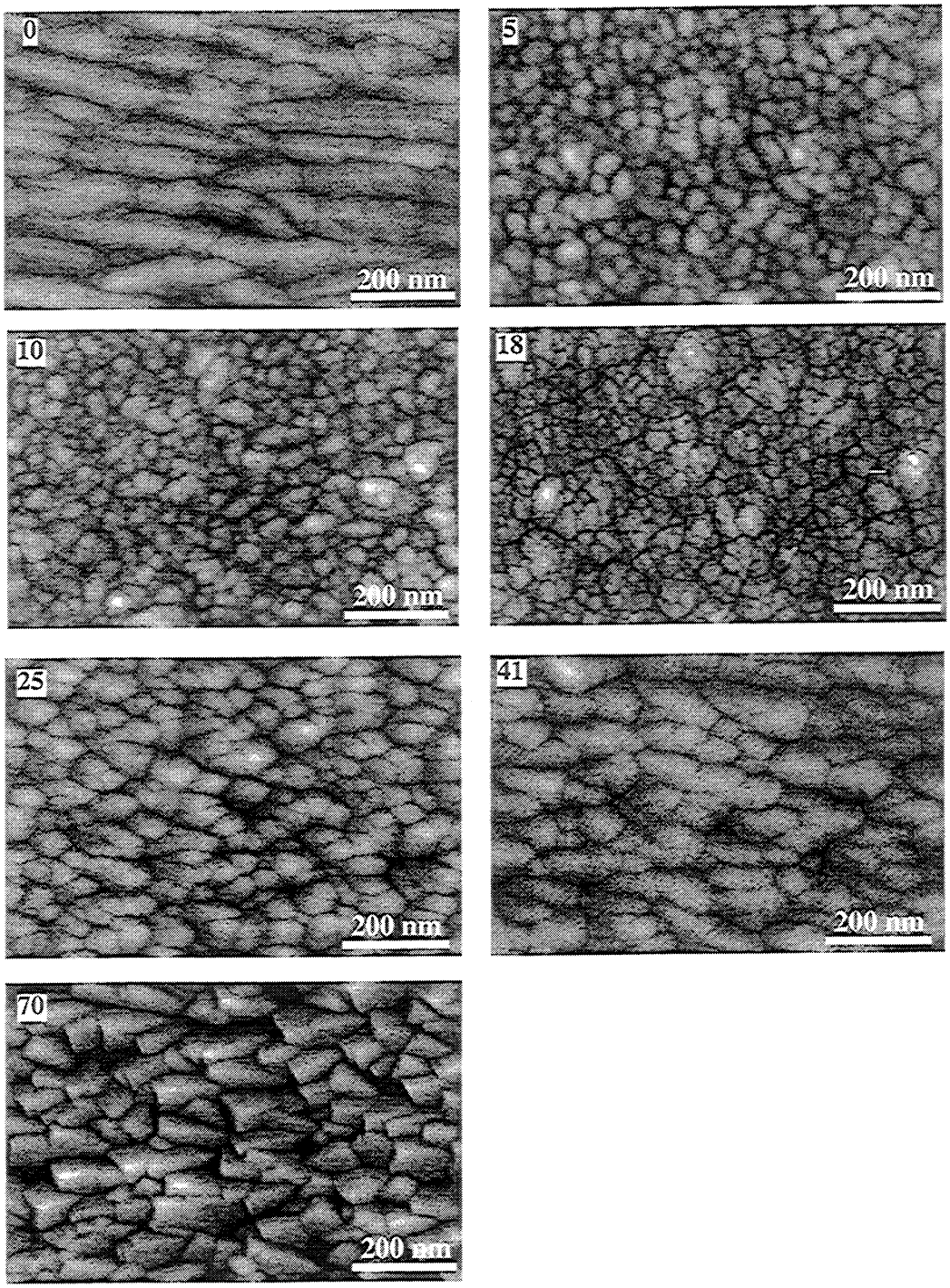


**Figure 15:** AFM micrographs showing the growth morphologies of chromium nitride films at varying nitrogen flows. All the films have the same nominal thickness: 1μm.

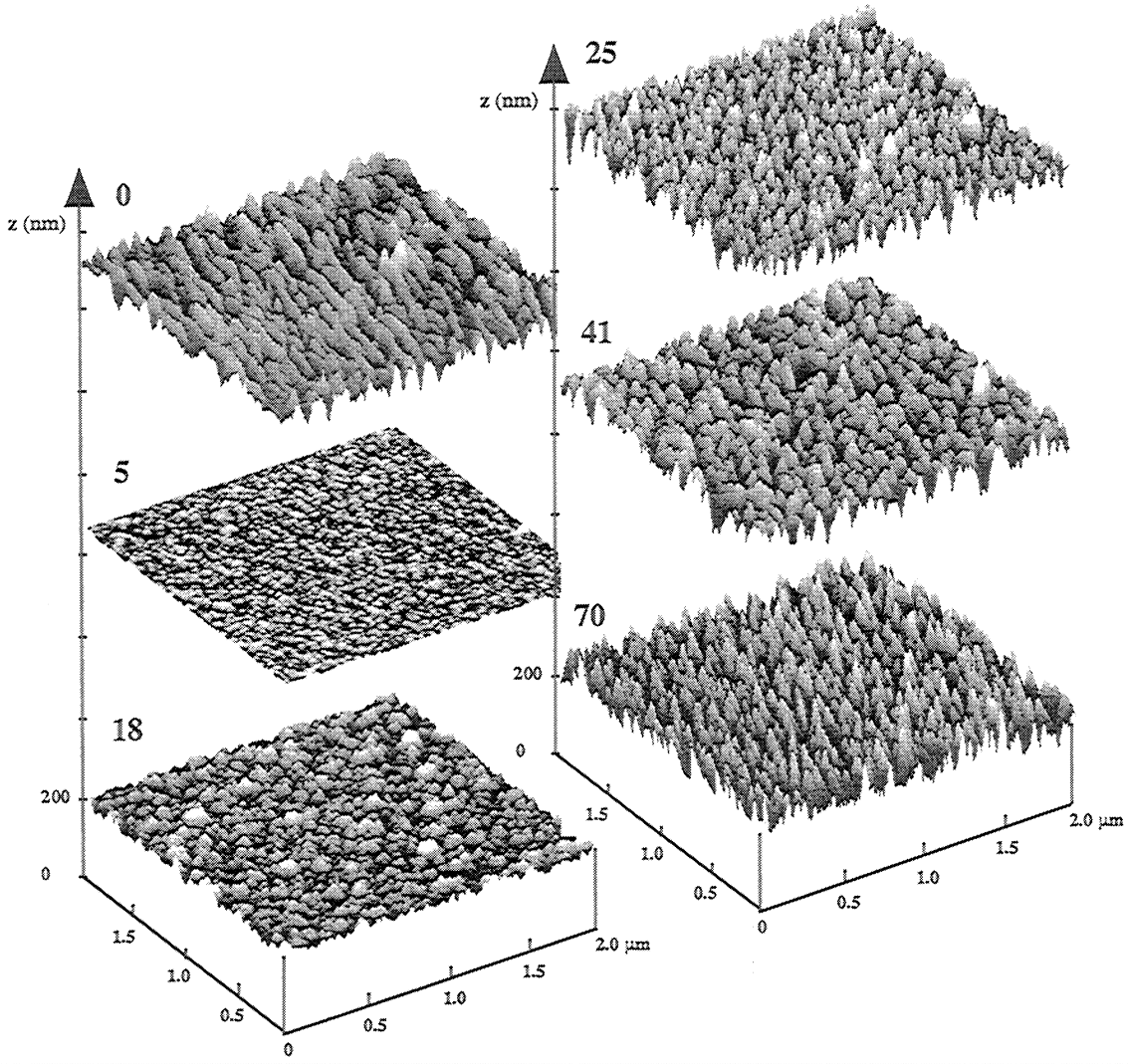


**Figure 16:** Surface plots of the AFM images showing the surface roughness at varying nitrogen flows.

## VI. Barrel Sputter Coater Depositions

A barrel coating matrix was conducted to investigate the effects of $N_2$ gas ratio and substrate biasing on the film phase (CrN vs. $Cr_2N$), crystal structure orientation, residual stress, coefficient of friction, and wear resistance. The matrix is shown in Table III.

**Table III:** Barrel Coating Matrix (run numbers)

| Gas Ratio ($Ar:N_2$) | -65V Bias | No Bias |
|---|---|---|
| 80:20 | B029 & B030 | B034 |
| 65:35 | B031 & B038 | B035 |
| 50:50 | B032 | B036 |
| 30:70 | B033 | B037 |

These runs were conducted under nominally the same parameters other than those listed in Table III. All runs were conducted at 2.5 millitorr overall pressure and had a chromium bond layer. The specific run conditions are listed in Table IV.

**Table IV:** Barrel Run Parameters

| Run # | Target Power (W) | Tumbling Period (sec) | Coating Time (hr) | Ar Flow (sccm) | $N_2$ Flow (sccm) | Ar Press. (%) | $N_2$ Press. (%) | Coat Bias (V) |
|---|---|---|---|---|---|---|---|---|
| B029 | 1000 | 44 | 2 | 35.8 | 9.5 | 80 | 20 | 64 |
| B030 | 1500 | 46 | 2 | 35.8 | 9.5 | 80 | 20 | 67 |
| B031 | 1000 | 45 | 4 | 23.8 | 15.0 | 65 | 35 | 51* |
| B038 | 1000 | 44 | 2 | 23.6 | 15.0 | 65 | 35 | 63 |
| B032 | 1000 | 45 | 4 | 20.5 | 20.0 | 50 | 50 | 65 |
| B033 | 1000 | 45 | 4 | 15.0 | 40.0 | 30 | 70 | 73 |
| B034 | 1000 | 44 | 4 | 35.8 | 9.5 | 80 | 20 | 0 |
| B035 | 1000 | 44 | 4 | 23.8 | 15.0 | 65 | 35 | 0 |
| B036 | 1000 | 44 | 4 | 20.7 | 20.3 | 50 | 50 | 0 |
| B037 | 1000 | 44 | 4 | 15.5 | 40.0 | 30 | 70 | 0 |

* Run B031 appeared to have biasing problems. Graphite dust found in bias assembly after run.

Residual stress in the barrel deposited films was monitored by measuring the deflection of steel witness coupons. These deflections are indicated in Table V along with the relevant deposition parameters. Positive deflections indicate compressive residual stresses in the films.

**Table V:** Barrel Residual Stress

| Run # | Target Power (W) | Coating Time (hr) | Ar Press. (%) | $N_2$ Press. (%) | Coat Bias (V) | Deflection (μm) |
|---|---|---|---|---|---|---|
| B029 | 1000 | 2 | 80 | 20 | 64 | 334 |
| B030 | 1500 | 2 | 80 | 20 | 67 | 292 |
| B031 | 1000 | 4 | 65 | 35 | 51* | 83 |
| B038 | 1000 | 2 | 65 | 35 | 63 | 125 |
| B032 | 1000 | 4 | 50 | 50 | 65 | 250 |
| B033 | 1000 | 4 | 30 | 70 | 73 | 417 |
| B034 | 1000 | 4 | 80 | 20 | 0 | 167 |
| B035 | 1000 | 4 | 65 | 35 | 0 | -208 |
| B036 | 1000 | 4 | 50 | 50 | 0 | 0 |
| B037 | 1000 | 4 | 30 | 70 | 0 | 250 |

* Run B031 appeared to have biasing problems. Graphite dust noted in bias assembly after run.

The residual stresses in the barrel films show close relationships to those reported for the Sloan system depositions. Higher compressive residual stresses are found in biased runs and thicker films (in accordance with Stoney's equation). The only anamoly are run B031, which is obviously a result of the problem with the substrate biasing system during that run. Thus, B031 shows a characteristic deflection more indicative of an unbiased run. The repeat run for B031, which was B038, was carried out with only half the original deposition time. Therefore, the thickness of the film is roughly half the thickness. Assuming the residual stress is linear with film thickness, as indicated by Stoney's equation, a representative deflection measurement would be 250 μm rather than the 125 μm reported. Therefore, we can conclude that the B038 film has typical residual stress compared with the other biased runs in the barrel shown in Table V.

The unbiased barrel depositions show low compressive stresses or even zero or low tensile stresses. These films show these low stresses because of their natural crystal structure, only. There is an anamolous result in run B037 where the measured deflection indicated a compressive residual stress on the order of the negatively biased runs. The source of this result is unclear.

## VI.A Barrel X-Ray Diffraction Results and the $Cr_xN$ Phase Field

**Table VI:** Barrel Coating Matrix – X-ray Results
Phase & Preferred Orientation (if any)

| Gas Ratio (Ar:$N_2$) | -65V Bias | No Bias |
|---|---|---|
| 80:20 | Cr + small CrN | Cr + small CrN |
| 65:35 | $Cr_2N$ | $Cr_2N$ + CrN |
| 50:50 | $Cr_2N$ + CrN | $Cr_2N$ (10·0) |
| 30:70 | $Cr_2N$ | $Cr_2N$ |

The x-ray results in Table VI indicate that in both the unbiased and biased (-65V) run conditions, low $N_2$ gas content (20% $N_2$) results in mostly chromium deposition with a small amount of CrN. This is reasonable since the there is little nitrogen available for the sputtered gas phase Cr to react with on the substrate surface. Meanwhile, for both biasing conditions at high $N_2$ content (70% $N_2$) only $Cr_2N$ is formed. This was an unexpected result since the chromium sputtering rate should have been significantly slowed down as a result of the only 30% argon content. Therefore, the chromium rich $Cr_2N$ should not have been favored and mostly CrN would be expected.

At intermediate gas ratios, the biased and unbiased conditions showed different results. For the biased condition, increasing the nitrogen content to 35% $N_2$ produced $Cr_2N$. Further increasing the $N_2$ content to 50% resulted in a mixed phase film of $Cr_2N$ and CrN. Meanwhile, at a nitrogen content of 35% in the unbiased condition, the mixed phase of $Cr_2N$ and CrN is immediately formed. Interestingly, at 50% $N_2$ content in the unbiased condition only $Cr_2N$ is formed but with a preferred out-of-plane texture in the (10·0) direction.

These results are contrary to previous reports of this program which stated that only pure CrN was formed in the barrel sputtering system. Evidently, the oscillating nature of the current depositions alter the dynamics of the crystal growth to produce a wide variety of structures in the $Cr_xN$ system, while the previous static depositions only formed CrN.

## VI.B Barrel Target Flux Distribution

A static deposition was conducted for one hour at 1000W target power, 2.5 millitorr pressure, and roughly 65:35 Ar to $N_2$ percentage in order to determine the barrel system sputtering rate as a function of position in the barrel chamber. Profilometry measurements were conducted on masked strips, ex situ, and the results are presented in Figure 17. The deposition rate is clearly nonuniform throughout the barrel with the maximum rate directly under the center of the target. There is a drop off in deposition rate along the centerline, relative to the maximum location. This is because the center flux is a combination of perpendicular flux from the center area of the target as well as off normal flux from adjacent areas of the target. Near the ends of the target there is obviously no off normal flux contribution from past the end of the target, resulting in less deposition rate. There is also a drop off in deposition rate from side to side in the barrel due to the same reason.

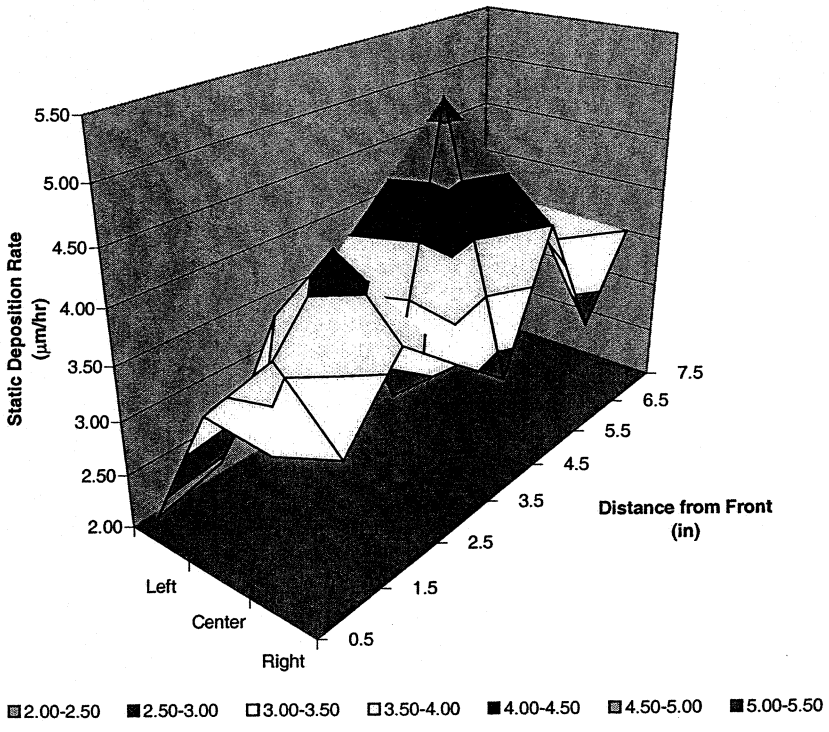


**Figure 17:** Deposition rate distribution in the barrel chamber (static).

## VI.C Barrel Film Coefficients of Friction

The barrel films were subjected to pin-on-disk friction and wear tests identical to those described in Section III.C. The friction results of these tests are indicated in Table VII.

**Table VII:** Barrel Coating Coefficients of Friction

| Gas Ratio ($Ar:N_2$) | -65V Bias | No Bias |
|---|---|---|
| 80:20 | 0.44 & 0.49[1] | 0.41[2] |
| 65:35 | Note 3 | 0.41 |
| 50:50 | 0.22 | 0.31 |
| 30:70 | 0.24 | Note 3 |

Note 1: This data is from a run with 1500W Cr target power, as opposed to the 1000W for the rest of the group. Both these data were rough tests.
Note 2: B034 conducted with no bias and 80:20 gas ratio was a rough test.
Note 3: B038 conducted with bias and a gas ratio of 65:35 as well as B037 conducted with no bias and 30:70 gas ratio had an immeasurable coefficients of friction since the tests were so rough.

Table VII indicated poor coefficients of friction for gas ratios of 80:20 in both the unbiased and biased conditions. This is clearly due to the high chromium content of the film, as shown by x-ray analysis, which was too soft for the test conditions. Immeasurable coefficients of friction were also the result for the 65:35 biased run and the 30:70 unbiased run. Both these coatings consisted of $Cr_xN$ phases. These coatings may have been rough or porous, leading to the extremely rough friction tests.

The rest of the friction results presented in Table VII were from fairly smooth tests. It is clear that the unbiased runs all had higher coefficients of friction than the biased runs. This is due to the harder, more dense structures of the biased films. Little difference in coefficient of friction is evident within the biased run group due to change in gas ratio. However, in the unbiased runs, increasing the nitrogen content from 35% to 50% had an effect of reducing the coefficient of friction from 0.41 to 0.31.

## VI.D Barrel Film Wear Resistance

After the friction and wear tests described above, optical microscope measurements were taken of the wear track widths on the samples and the pin wear scar width on the WC-Co balls. These give quantitative numbers for wear resistance comparisons.

**Table VIII:** Barrel Coating Wear Measurements
track wear (mm)
*pin wear (mm)*

| Gas Ratio ($Ar:N_2$) | -65V Bias | No Bias |
|---|---|---|
| 80:20 | 0.42 & 0.37[1]<br>*0.41 & 0.26*[1] | 0.41[2]<br>*0.41*[2] |
| 65:35 | 0.34 & 0.22[3]<br>*0.30 & 0.21*[3] | 0.27<br>*0.27* |
| 50:50 | 0.28<br>*0.16* | 0.19<br>*0.20* |
| 30:70 | 0.19<br>*0.20* | 0.28[3]<br>*0.23*[3] |

Note 1: This data is from a run with 1500W Cr target power, as opposed to the 1000W for the rest of the group. Both these data were rough tests.
Note 2: B034 conducted with no bias and 80:20 gas ratio was a rough test.
Note 3: B038 conducted with bias and a gas ratio of 65:35 as well as B037 conducted with no bias and 30:70 gas ratio had an unmeasurable coefficients of friction since the tests were so rough.

The track wear and corresponding pin wear for all of the barrel coatings were roughly equivalent, indicating the film hardness was comparable to the hardness of the WC-Co balls. The only exception was the biased run B032 conducted at 50% $N_2$ gas content.

The wear measurements indicated in Table VIII correspond well with the coefficients of friction of Table VII. The high coefficients of friction for the 80:20 runs have the highest wear widths. The lowest wear widths correspond to the lower coefficients of friction, namely B033 and B036. However, the track width for the biased 50:50 run, B032, was higher than B033 which had a similar coefficient of friction.

The trend of lower coefficient of friction with increasing $N_2$ content among the unbiased runs is again indicated in the wear measurements. The lower coefficients at higher $N_2$ content resulted in smoother contact and lower wear on both the flat and pin.

## VII. Conclusions

The past year has involved extensive characterization of RF and DC sputtered $Cr_xN$ films. The major conclusions are the following.

- Reliable working gas partial pressure control requires a Residual Gas Analyzer (RGA) rather than flow meters.
- An RGA measured argon/nitrogen partial pressure ratio of 65/35 with 600W target power gives good tribological results in the Sloan system at substrate distances of 3.5 inches.
- RF sputtered CrN films show random crystal orientation.
- DC sputtered $Cr_2N$ films with exhibit (10·0) out-of-plane texture.
- Increased compressive residual stress in CrN films has been observed with the application of a negative substrate bias near 50W. These films had good to excellent hardness and wear resistance.
- RF sputtered CrN films show coefficients of friction near 0.50
- DC sputtered CrN films show coefficients of friction near 0.20
- Super-stoichiometric $CrN_{1+x}$ films can be formed with excess $N_2$ in the chamber, as shown by the lattice expansion of the Michigan films.
- Super-stoichiometric $CrN_{1+x}$ increases the compressive residual stress component in the films.
- Mixed phase CrN films showed a more equiaxed grain structure, less texture, and less mesoscale roughness. These smoother surfaces may be desirable for tribological applications despite lower hardness.